

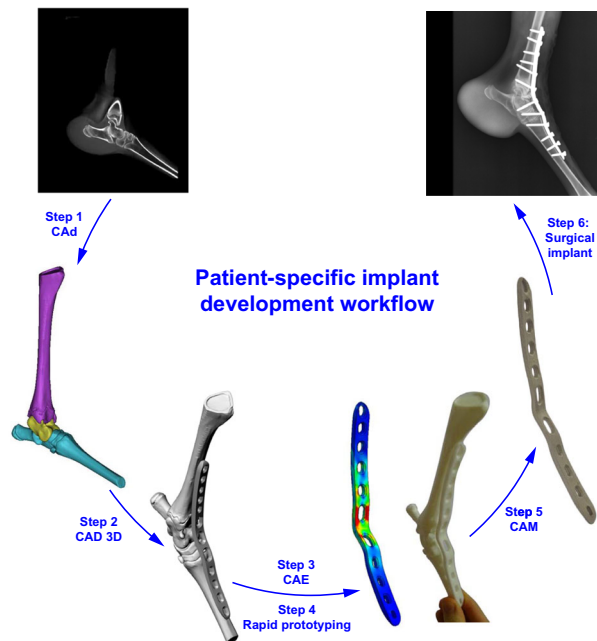


3D printing of patient-specific 316L–stainless–steel medical implants using fused filament fabrication technology: two veterinary case studies

J. M. Chacón¹ · P. J. Núñez¹ · M. A. Caminero¹ · E. García-Plaza¹ · J. Vallejo¹ · M. Blanco²

Received: 7 February 2022 / Accepted: 22 April 2022 / Published online: 2 June 2022
© The Author(s) 2022

Graphic abstract



Biomedical fracture fixation implants have complex sculptured geometries to adapt perfectly to fractured bones, making them difficult and expensive to manufacture with conventional machining methods. Fused filament fabrication (FFF) is a very popular Additive Manufacturing technology

that simplifies the manufacture of parts with complex geometries, making it ideal for the manufacture of customized medical implants. The use of FFF-based new engineering biocompatible thermoplastic materials, such as PEEK or 316L hybrid metal–polymer opens new possibilities for the manufacture of patient-specific biomedical implants using standard computer-aided technology (CAX), and FFF-based 316L stainless steel manufacturing with subsequent debinding and sintering stages. The goal was to establish a systematic workflow for the 3D manufacturing of biomedical fracture fixation implants. The

✉ J. M. Chacón
jesusmiquel.chacon@uclm.es

¹ Escuela Técnica Superior de Ingeniería Industrial, Universidad de Castilla-La Mancha, Avda. Camilo José Cela, 2, 13071 Ciudad Real, Spain

² Protresde Ingeniería y Soluciones, C/Solana 60, nave 3, 13005 Ciudad Real, Spain

contribution was twofold, both in conceptual and procedural terms. The proposed CAx workflow was successfully applied to two veterinary case studies, which confirmed the suitability of the customized biocompatible AISI 316L stainless steel biomedical implants processed by FFF technique.

Introduction

Patient-specific implants mimic the anatomy of the defective area in a patient; hence, they usually exhibit complex sculptured surfaces. Customized fracture-fixation implants can be produced by conventional manufacturing methods. However, the machining of complex sculptured surfaces of customized implants entails a high cost and is a time-consuming process.

Recently, additive manufacturing (AM) has made significant advances in biomedicine with the design, development, and fabrication of personalized medical implants—this underscores the potential of AM [1]. For example, the AM of customized porous Ti6Al4V scaffolds using selective laser melting (SLM) has been successfully developed at the Biofabrication Laboratory of Sichuan University [2] for human and veterinary clinical studies [3, 4]. These 3D-printed porous scaffolds are ideal for bone tissue engineering for bone osteointegration [5, 6]. The AM of patient-specific implants has become a well-established method that gives results similar to those of conventional manufacturing processes and materials [7].

The objective of this study is to assess an innovative workflow for the design and manufacturing of patient-specific biomedical stainless-steel implants. The proposed workflow integrates standard computer-aided technologies (CAx) with fused filament fabrication (FFF) AM technology, with subsequent debinding and sintering stages. Moreover, the proposed methodology can be applied to different metal AM technologies.

A commercially available Ultrafuse[®] stainless-steel 316L metal-polymer filament supplied by BASF [8] was employed to manufacture different implants with a low-cost 3D printer. The topic of this study, relating to surgical implants and guides, falls well within the five major areas of AM applications in the medical sector [9]. The advantages of the FFF-based stainless-steel AM technique do not lie in the enhancing of the mechanical performance of a material by improving density levels, as is the case in other techniques, but in providing a cost-effective method for manufacturing near-dense metal implants with acceptable mechanical properties [10].

Thus, the proposed workflow is based on the following CAx techniques: anatomical reconstruction (CAD), design (3D CAD), mechanical and geometrical validation (CAE), and manufacturing (CAM). The integration of CAx and

FFF-based AM technology has enabled the design of patient-specific implants with complex sculptured geometries and a high degree of flexibility. CAx and FFF-based AM technologies provide an ideal fit for customized implants, as well as prevent injury and maximize patient comfort, which is one of the needs that has been identified for AM prosthetic applications [11].

Proposed workflow via CAx and FFF

One of the main drawbacks in the design and manufacture of patient-specific medical implants is that the whole process is time consuming. However, the process has been reduced, through recent research and innovation, to a few hours or days rather than weeks [12], which is essential for carrying out urgent medical interventions. Our proposed workflow explores the use of computer-aided techniques (CAx) in conjunction with FFF-based AM technology. CAx, extensively used in the field of mechanical engineering [13], can significantly reduce design and product development time as well as costs because CAx is capable of the real-time detection and correction of design errors. Moreover, FFF-based AM technology enables the manufacturing of products with complex sculptured geometries with reduced production time and costs due to lower material wastage.

The proposed workflow for the design and manufacture of customized implants was divided into six steps, as shown in Fig. 1:

- *Step 1* Digital anatomical reconstruction of the fractured bone via a computer-aided diagnosis (CA_d) system.
- *Step 2* Development of a patient-specific bio-designed implant using computer-aided design (CAD 3D).
- *Step 3* Mechanical validation using computer-aided engineering (CAE) via finite element method (FEM) analysis.
- *Step 4* Geometrical validation via rapid prototyping using thermoplastic materials.
- *Step 5* FFF of the metal implant using an AM computer-aided manufacturing (CAM) system and finishing operations.
- *Step 6* Surgical patient-specific prosthesis implant.

The proposed workflow was applied in two veterinary case studies, i.e., a canine cranial plate, and a lamb dorsal pantarsal arthrodesis plate. This study focuses on steps 1, 2, and 5 that concern the bio-design and manufacturing process.

Anatomic reconstruction and implant design

Anatomic reconstruction via CAD

The design process of a patient-specific fracture fixation begins with capturing the geometry and dimensions of the fractured bone and the area where the implant is to be placed. As direct measurements are not possible in medical applications, computer-aided diagnosis with a medical imaging (CAD) system is required to utilize medical imaging techniques to determine the anatomical geometry of the patient.

The CAD system combines a computed tomography (CT) scan and reverse engineering for 3D anatomy reconstruction. The CT scan provides the geometry of the affected part. As a result, a Digital Imaging and Communications in Medicine (DICOM) file is obtained. Next, reverse engineering generates a 3D virtual model of the affected bone

for use in computer-aided design. Thus, a point cloud of the geometry is obtained, and the 3D model is represented as a triangular-faced mesh, such as in a stereolithography (STL) format, that lacks topological information. This data conversion from DICOM to STL requires a process referred to as image segmentation.

Thresholding is the most common technique used for image segmentation [14] and to capture the bone structure excluding the surrounding soft tissue. The medical images contained in the DICOM files were stored in a grayscale image. Thresholding technique segments an image by detecting pixels with an intensity value within the user-selected threshold range.

In this workflow, the computer-aided diagnosis CAD software *Materialise Mimics* was used to convert the DICOM data into a 3D STL virtual model of the affected bone that was directly transferred to a computer-aided design system.

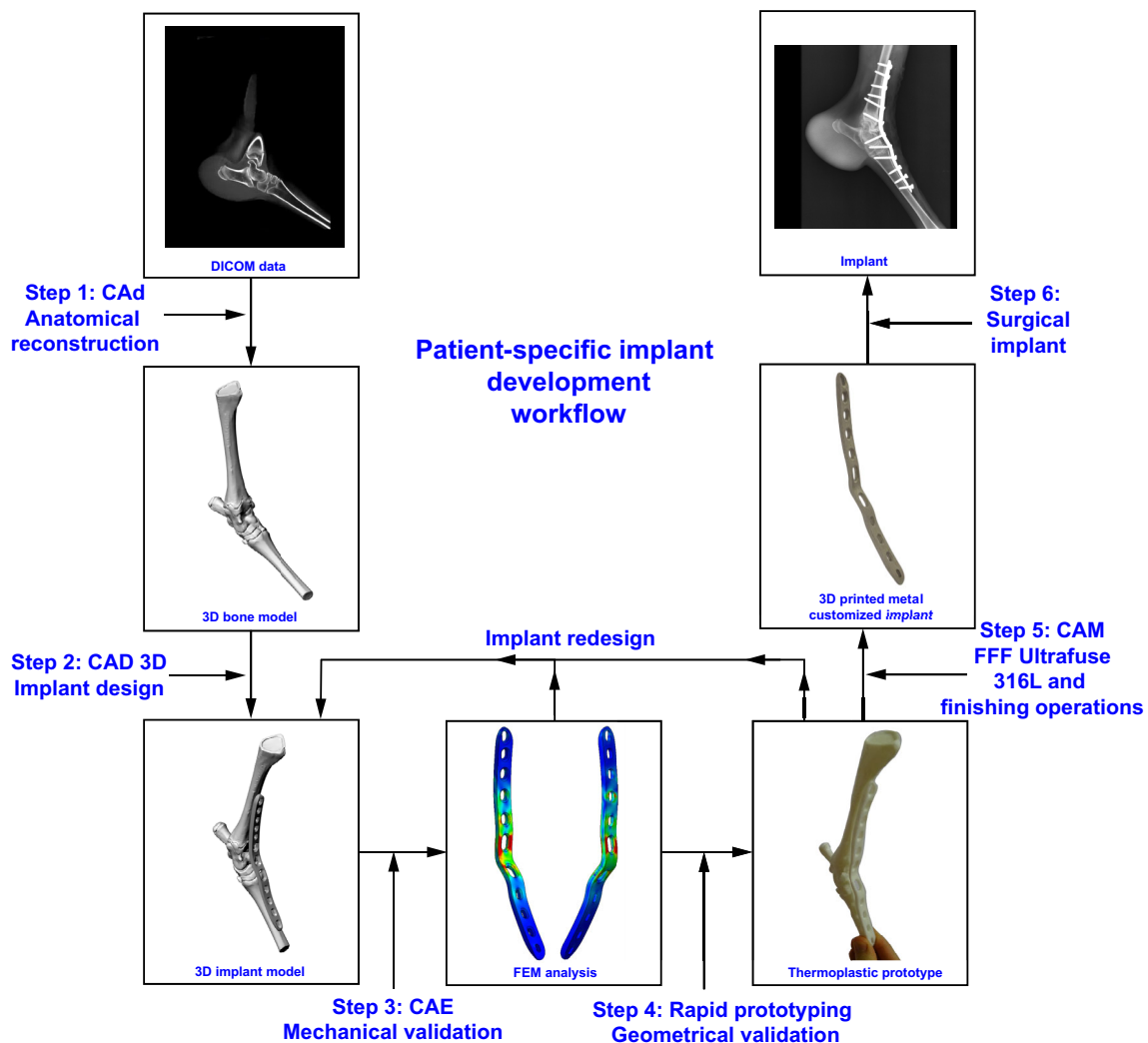


Fig. 1 Workflow diagram depicting the implant development process

For global thresholding, *Mimics* offers standard, predefined threshold ranges for individual tissue identification. Moreover, *Mimics* enables the local threshold range to be selected manually in a graphical way.

Image segmentation involves the global thresholding of a DICOM file. First, the DICOM file was imported from *Mimics*. Next, the digital images were segmented using the standard, predefined threshold range “Compact Bone”. This method effectively yielded a 3D polygon model. However, all the bones were segmented together in only one group rather than individually or by blocks, making it difficult to prototype the model and modify it later.

As accurate segmentation of complex anatomical regions often requires manual segmentation, a local threshold was generated by defining various threshold ranges for different parts of the image. In *Mimics*, this process was performed with the function “profile line”, where the user draws a line crossing the region to be segmented. The threshold range was defined with maximum and minimum values contained within the drawn line. This process was more complex than automated global segmentation, but the reconstructed models were faithful to the anatomy of the affected bone. Moreover, a segmentation by blocks was generated, which allowed for subsequent modifications in the design process of the fixation implant. Finally, the DICOM to STL conversion was performed before it was later imported into a CAD 3D system.

Patient-specific implant design via CAD 3D

The most important component of computer-aided diagnosis (CAD) is the obtaining of an accurate capturing of bone structures. However, this precision is useless if it is not employed to design a precise patient-specific fracture-fixation implant. Computer-aided design systems provide tools such as non-uniform rational B-splines (NURBS) [15] capable of dealing with this complexity. NURBS provides the flexibility required to design implants fully adapted to a patient’s geometry.

As result of the anatomic reconstruction, a 3D STL model was obtained that was represented as a triangular-faced mesh. Out of the many commercial programs on the market, *Rhino3D* was chosen for its versatility. *Rhino3D* is a commercial NURBS-based CAD 3D package that also admits and supports point clouds and polygon meshes, which makes it a fundamental tool for combining computer-aided diagnosis (CAI) with computer-aided design (CAD 3D).

The implant design began by the importing of the STL anatomical model into *Rhino3D*. Following the indications of the medical staff, the reconstructed model was modified in order to place the fractured bones into their proper positions. To perform this modification, the model had to have the necessary degrees of freedom, which was achieved by computing local segmentation by blocks.

First, a 3D geometry of the fixation implant was extracted from the surface of the bone reconstruction model. Next, a final design of the patient-specific implant was generated, taking into account parameters directly affecting the dimensions of the fixation implant, such as number, size, position, and orientation of the screw holes.

FFF of metal implants using the AM system

The implant was manufactured after validating the design of the implant with the CAE analysis and prototyping phase (steps 3 and 4). This workflow permitted the manufacturing of customized metal implants with a low-cost, dual-extruder FFF 3D printer, and commercially available BASF Ultrafuse® 316L metal–polymer composite filament [8]. In this step, *Ultimaker Cura* [16] was used as the additive manufacturing CAM software. Optimal FFF process parameters were selected to improve mechanical performance in the vertical direction [17]. The metal implant obtained from the FFF 3D printer, denoted as the green part, was post-processed using commercially available BASF catalytic debinding and sintering stages [18].

The mechanical performance of the fixation implants depended on the AM build orientation. The optimum orientation of specific patient implants was found to be in the flat or on-edge orientation as the main loading direction was parallel to the build layers, which agrees with the observations of other authors [19].

The FFF-based manufacturing process associated with the debinding and sintering stages resulted in anisotropic shrinkage. For this reason, the filament manufacturer recommends using three different oversizing factors (OSF) for each of the main directions of the part [8]: $OSF_X = OSF_Y = 1.20$ and $OSF_Z = 1.25$.

In order to manufacture more precise parts, the crucial importance to patient-specific medical implants of the measurement of the shrinkage of 3D-printed 316L stainless-steel sintered parts, has been shown in a previous study [10]. The obtained results reveal an average anisotropic shrinkage of 18% on the X- or Y-axis, and 21% on the Z-axis.

Finally, the post-processing stage involved surface grinding and electro-polishing of the as-built patient-specific implants in order to reduce the number of surface defects.

Veterinary case studies

Two veterinary cases of customized implants manufactured using FFF were assessed. Both clinical veterinary case studies were carried out in collaboration with the Veterinary Hospital of Ciudad Real (Spain).

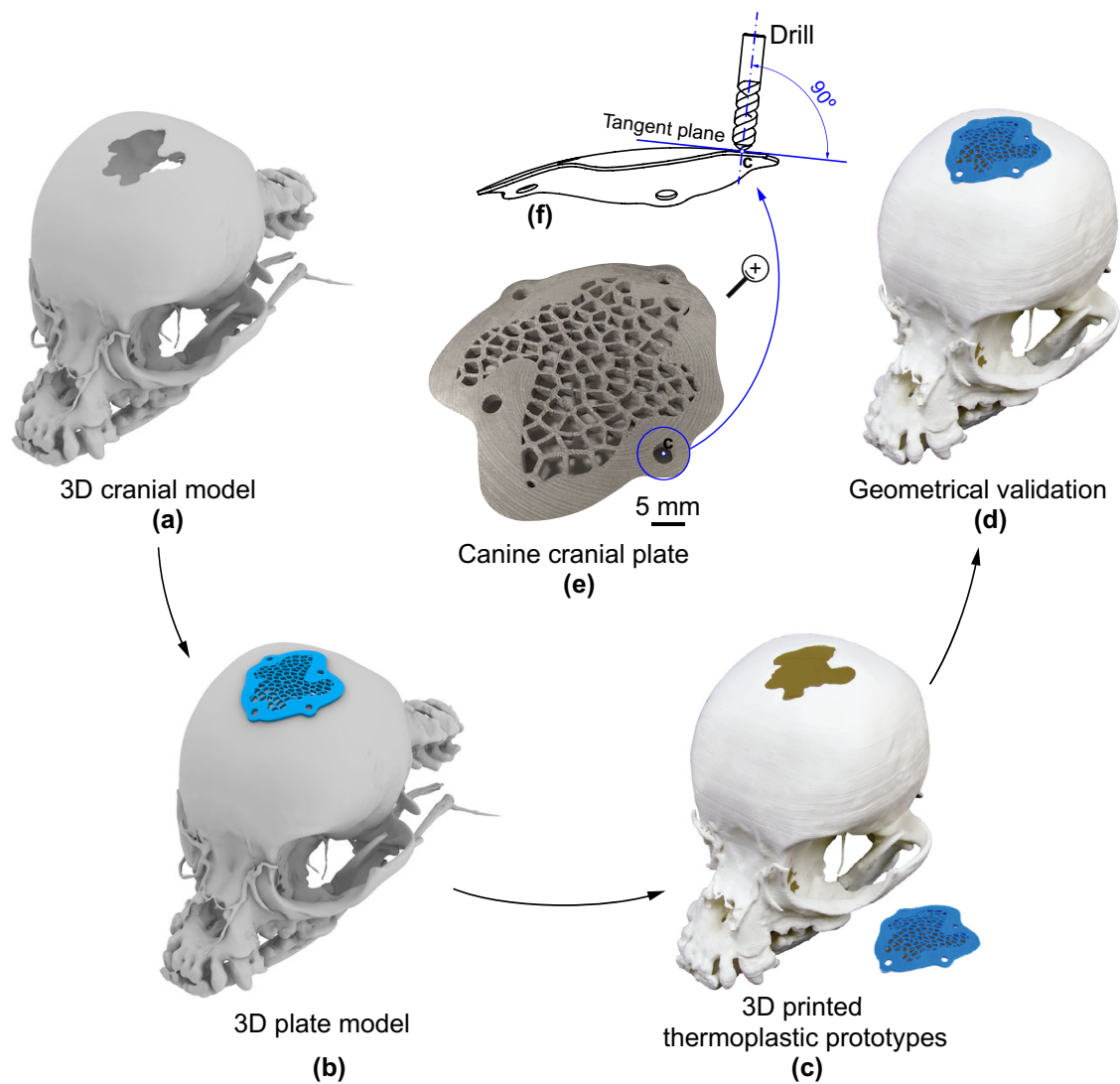


Fig. 2 FFF of the 316L stainless-steel canine cranial plate: **a–d** design and validation, and **e** 3D-printed metal cranial plate. **f** Detail of the fixing hole direction

Canine cranial implant

The first case study involved a cranial implant in a poodle following an accidental fall. After examination, the animal was diagnosed with a fractured and collapsed skull and severe brain trauma. As repositioning of the bone fragments into the correct place was not possible, the veterinary team decided to place a customized cranial plate adapted to the shape of the skull. In this study, a canine cranial implant was manufactured with the FFF technique in order to reduce fabrication costs.

The design and manufacture of a customized canine cranial implant began with the anatomical reconstruction of the fractured bones (Fig. 2a). As this type of implant was neither designed to fix any joints, nor to be subjected to great stresses throughout its useful life—except for occasional impacts, the final design was simplified (Fig. 2b) in the following way:

1. Design of the central area using a mesh structure to obtain a lightweight structure and to save manufacturing costs, which was possible due to the flexibility of the FFF process.
2. Fixation of the plate with four 2-mm-diameter screws, the minimum number of screws recommended [20].

Next, two polylactic acid (PLA) prototypes of the plate and a cranial model (Fig. 2c) were manufactured in step 4 for geometric validation purposes (Fig. 2d). Finally, the cranial plate was additively manufactured (Fig. 2e). In accordance with the guidelines of the veterinary team, the fixing holes were drilled perpendicular to the tangent plane at the center *C* of the holes of the implant surface (see detail in Fig. 2f).

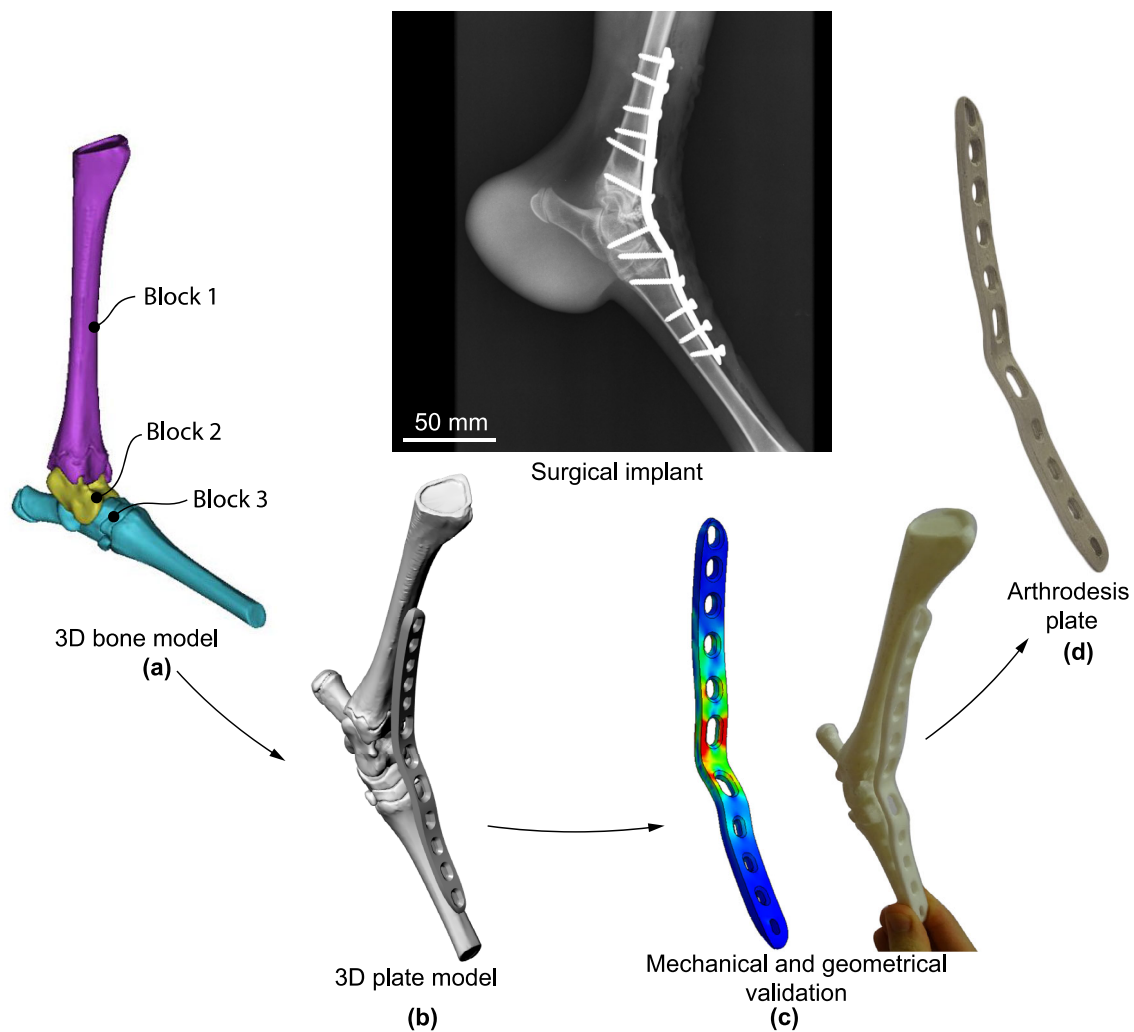


Fig. 3 FFF of a 316L-stainless-steel arthrodesis plate: **a–c** design and validation and **d** 3D-printed metal arthrodesis plate

Dorsal pantarsal arthrodesis plate

The second case study involved the fabrication of a dorsal pantarsal arthrodesis plate with the goal of repairing a rupture of the gastrocnemius tendon in a lamb. Due to the anatomical differences in limb bone structures between dogs and lambs, a standard-size implant could produce bone fractures in the affected limb. Moreover, the reshaping of a fixation plate could be inefficient and inaccurate [21].

Moreover, the commercial dog implant required screws too large for the bone structure of a lamb. To overcome these hurdles, veterinary cuttable plates (VCPs) for pantarsal arthrodesis in cats were employed [22], as a VCP could be easily adapted to the anatomy of a lamb. As VCPs are relatively weak in flexural strength, they are recommended for dorsal plating where the plate is positioned on the compression side of the joint. Thus, the veterinary team decided to

use a customized dorsal pantarsal arthrodesis plate adapted to the limb.

In step 1, in order to provide the necessary degrees of freedom to modify the bones of the limb to achieve the proper angle, local segmentation in three blocks was performed (Fig. 3a). In the case of the dorsal plate, the implant had to be fixed to the tibia, talus, calcaneus, and tarsus. Screw position and orientation were decided by the veterinary team in order to reduce the risk of screw cut-out [21]. The customized dorsal pantarsal arthrodesis plate was designed taking these factors into account (Fig. 3b).

As this type of plate is usually subjected to biomechanical stresses, its mechanical behavior was analyzed (step 3) via FEM prior to the manufacturing stage. Mechanical validation via FEM was performed using experimental results previously obtained by the authors [10]. The average

mechanical strength and stiffness values were used to simulate the mechanical performance of the implant via FEM. Moreover, in order to validate the final design of the plate and plan the surgical procedure according to step 4, a prototype of the plate was manufactured. Figure 3c shows the result of the mechanical and geometrical validation. Finally, the customized arthrodesis plate was manufactured after applying the FFF-based process combined with debinding and sintering described in step 5 (Fig. 3d). Figure 3 shows an X-ray image showing the plate in the correct position, and the plate adapting perfectly to the bone structure.

Conclusions

We assessed the integration of FFF technology into a CAx workflow with the aim of reducing the manufacturing costs and time of patient-specific fracture fixation implants. FFF combined with debinding and sintering offers a cost-effective technology for the manufacturing of metal parts. Moreover, CAx reduces design time and in turn patient-specific development time and costs. The workflow in this study enabled the manufacture of customized metal implants with a low-cost, FFF 3D printer, and commercial Ultrafuse® 316L stainless-steel/polymer composite filament. The precision of the entire AM process, including FFF printing, debinding, and sintering stages, is superior in precision to anatomic reconstruction via CAx. Hence, the precision of the AM process is not a limiting factor in the manufacture of patient-specific implants.

This innovative method was applied to two veterinary case studies. The results of this study corroborated the feasibility and potential of FFF technology for the manufacture of patient-specific biomedical implants.

Acknowledgements This research was supported by the Spanish Ministerio de Ciencia e Innovación and Junta de Comunidades de Castilla-La Mancha, under research grants PID2019-104586RB-I00, SBPLY/19/180501/000247 and SBPLY/19/180501/000170, funded by MCIN/AEI/10.13039/501100011033. The authors thank TRIDITIVE Company and Veterinary Hospital of Ciudad Real (Spain) for their technical support.

Author contributions JMC, PJN and MAC curated the data and contributed to conceptualization, formal analysis, methodology, investigation, and writing—original draft; EGP contributed to formal analysis, methodology, and writing—reviewing and editing; JV and MB contributed to formal analysis, software, and methodology.

Funding Open Access funding provided thanks to the CRUE-CSIC agreement with Springer Nature.

Declarations

Conflict of interest The authors declare that they have no conflict of interest.

Ethical approval This article does not contain any studies with human or animal subjects performed by any of the authors. The DICOM files and X-ray images were provided with permission from the Veterinary Hospital of Ciudad Real (Spain).

Open Access This article is licensed under a Creative Commons Attribution 4.0 International License, which permits use, sharing, adaptation, distribution and reproduction in any medium or format, as long as you give appropriate credit to the original author(s) and the source, provide a link to the Creative Commons licence, and indicate if changes were made. The images or other third party material in this article are included in the article's Creative Commons licence, unless indicated otherwise in a credit line to the material. If material is not included in the article's Creative Commons licence and your intended use is not permitted by statutory regulation or exceeds the permitted use, you will need to obtain permission directly from the copyright holder. To view a copy of this licence, visit <http://creativecommons.org/licenses/by/4.0/>.

References

1. Salmi M (2021) Additive manufacturing processes in medical applications. *Materials* 14(1):191. <https://doi.org/10.3390/ma14010191>
2. Zhou C, Wang K, Sun Y et al (2021) Biofabrication (3D Bioprinting) Laboratory at Sichuan University. *Bio-des Manuf* 4:432–439. <https://doi.org/10.1007/s42242-020-00115-2>
3. Yi T, Zhou C, Ma L et al (2020) Direct 3-D printing of Ti-6Al-4V/HA composite porous scaffolds for customized mechanical properties and biological functions. *J Tissue Eng Regen Med* 14:486–496. <https://doi.org/10.1002/term.3013>
4. Pei X, Wu L, Zhou C et al (2021) 3D printed titanium scaffolds with homogeneous diamond-like structures mimicking that of the osteocyte microenvironment and its bone regeneration study. *Biofabrication* 13:015008. <https://doi.org/10.1088/1758-5090/abdb89>
5. Pei X, Wu L, Lei H et al (2021) Fabrication of customized Ti6Al4V heterogeneous scaffolds with selective laser melting: optimization of the architecture for orthopedic implant applications. *Acta Biomater* 126:485–495. <https://doi.org/10.1016/j.actbio.2021.03.040>
6. Lei H, Yi T, Fan H et al (2021) Customized additive manufacturing of porous Ti6Al4V scaffold with micro-topological structures to regulate cell behavior in bone tissue engineering. *Mater Sci Eng C* 120:111789. <https://doi.org/10.1016/j.msec.2020.111789>
7. Tahayeri A, Morgan M, Fugolin AP et al (2018) 3D printed versus conventionally cured provisional crown and bridge dental materials. *Dent Mater* 34(2):192–200. <https://doi.org/10.1016/j.dental.2017.10.003>
8. BASF (2022) Ultrafuse® 316L. <https://forward-am.com/material-portfolio/ultrafuse-filaments-for-fused-filaments-fabrication-fff/metal-filaments/ultrafuse-316l/>. Accessed 4 Feb 2022
9. Tuomi J, Paloheimo KS, Vehviläinen J et al (2014) A novel classification and online platform for planning and documentation of medical applications of additive manufacturing. *Surg Innov* 21:553–559. <https://doi.org/10.1177/1553350614524838>
10. Caminero MA, Romero A, Chacón JM et al (2021) Additive manufacturing of 316L stainless-steel structures using fused filament fabrication technology: mechanical and geometric properties. *Rapid Prototyp J* 27(3):583–591. <https://doi.org/10.1108/rpj-06-2020-0120>
11. Huang Y, Schmid SR (2018) Additive manufacturing for health: state of the art, gaps and needs, and recommendations. *J Manuf Sci Eng* 140(9):94001. <https://doi.org/10.1115/1.4040430>

12. Tilton M, Lewis GS, Manogharan GP (2018) Additive manufacturing of orthopedic implants. In Li B, Webster T (eds) *Orthopedic biomaterials*, Springer, Cham, pp 21–55. https://doi.org/10.1007/978-3-319-89542-0_2
13. Mircheski I, Lukaszewicz A, Szczebiot R (2019) Injection process design for manufacturing of bicycle plastic bottle holder using CAX tools. *Procedia Manuf* 32:68–73. <https://doi.org/10.1016/j.promfg.2019.02.184>
14. Castellano G, Bonilha L, Li L et al (2004) Texture analysis of medical images. *Clin Radiol* 59(12):1061–1069. <https://doi.org/10.1016/j.crad.2004.07.008>
15. Farin G (1999) *NURBS from projective geometry to practical use*, 2nd edn. AK Peters, Natick
16. Ultimaker (2022) Ultimaker Cura. <https://ultimaker.com/software/ultimaker-cura>. Accessed 2 Feb 2022
17. Chacón JM, Caminero MA, Núñez PJ et al (2021) Effect of nozzle diameter on mechanical and geometric performance of 3D printed carbon fibre-reinforced composites manufactured by fused filament fabrication. *Rapid Prototyp J* 27(4):769–784. <https://doi.org/10.1108/rpj-10-2020-0250>
18. BASF AG (2003) *Catamold® Feedstock for metal injection molding: processing–properties–applications*. Technical Information, pp 1–13
19. Tilton M, Armstrong A, Sanville J et al (2020) Biomechanical testing of additive manufactured proximal humerus fracture fixation plates. *Ann Biomed Eng* 48:463–476. <https://doi.org/10.1007/s10439-019-02365-3>
20. Johnson AL, Houlton J, Vannini R (2005) *AO principles of fracture management in the dog and cat*. Thieme Publishing Group, New York
21. Tilton M, Lewis GS, Wee HB et al (2020) Additive manufacturing of fracture fixation implants: design, material characterization, biomechanical modelling and experimentation. *Addit Manuf* 33:101137. <https://doi.org/10.1016/j.addma.2020.101137>
22. Salvatierra DNA, Witte PG, Scott HW et al (2018) Partansal arthrodesis in cats using orthogonal plating. *J Feline Med Surg* 20(1):45–54. <https://doi.org/10.1177/1098612x17698264>